MONITORING OF IONOSPHERIC SCINTILLATION PHENOMENA USING SYNTHETIC APERTURE RADAR (SAR)

S. Mohanty [1]*, C. Carrano [2], G. Singh [1]

[1] Centre of Studies in Resources Engineering, Indian Institute of Technology Bombay, Mumbai, India (shradha_mohanty, gulab.singh)@iitb.ac.in
[2] Institute for Scientific Research, Boston College, Newton, MA, USA – charles.carrano@bc.edu

Commission V, SS: Atmosphere, Ocean, Weather and Climate

KEY WORDS: Ionosphere, scintillations, synthetic aperture radar (SAR), total electron content (TEC), amplitude scintillation (S_4)

ABSTRACT:

The applications of synthetic aperture radars (SAR) have increased manifold in the past decade, which includes numerous Earth observation applications such as agriculture, forestry, disaster monitoring cryospheric- and atmospheric- studies. Among them, the potential of SAR for ionospheric studies is gaining importance. The susceptibility of SAR to space weather dynamics, and ionosphere in particular, comes at low frequencies of L- and P-bands. This paper discusses one such scintillation event that was observed by L-band Advanced Land Observation Satellite (ALOS)-2 Phased Array L-type SAR (PALSAR) over southern India on March 23, 2015. The sensors also acquired data sets on four other days on which the ionosphere was quiet. Ionospheric parameter measurements of total electron content (TEC) and amplitude scintillation (S_4) index from ground-based Global Navigation Satellite System (GNSS) receiver at Tirunelveli was used to establish the ionospheric conditions on the days of SAR acquisition as well as to corroborate the S_4 estimated from SAR. Multi-temporal ALOS-2 data sets were utilized to calculate S_4 from two separate methods and the results have a good agreement with GNSS receiver measurements. This highlights the potential of SAR as an alternate technique of monitoring ionospheric scintillations that can be utilized as complementary to the highly accurate and dedicated measurements from the GNSS networks.

1. INTRODUCTION

With the advent of spaceborne remote sensing, the spectrum of techniques for Earth observation has broadened. Adding to the list is synthetic aperture radar (SAR). The several advantages of SAR over other remote sensing techniques, such as all-weather- and day-night capability, penetration through the clouds, etc., makes it suitable for various applications. Agriculture, forestry, disaster monitoring, oceanic-, cryospheric- and atmospheric-studies are a few applications that are being widely implemented using SAR. The susceptibility of SAR to space weather dynamics comes from its interaction with the charged layer of free electrons, the ionosphere. SAR sensors operating at low frequency bands of L-band (~1.27 GHz) and P-band (~450 MHz) are vulnerable to this charged layer in the atmosphere.

1.1 Ionosphere- An introduction

The ionosphere is defined as the layer of the Earth's atmosphere that forms an interface between the inner atmosphere and the outer space. Although the exact extent of the ionosphere is not clearly defined, it can be said to extend from nearly 50-500 kms and above (IEEE 1998). It is formed by the process of ionization of neutral molecules by solar and cosmic radiations. The presence of weakly ionized plasma (consisting of free electrons and ions) in the ionosphere enables trans-ionospheric radio communication and navigation systems to operate (Cannon and et al. 2013). Historically, these techniques have been widely explored for ionospheric scintillation research benefitting fields like atmospheric physics, geophysics, ocean acoustics, astronomy, radio physics, etc. Conversely, the charged layer also responsible for the different types of signal degradation in these systems (Carrano, Bridgwood and Groves 2009). The impact of the ionosphere on technologies relying on trans-ionospheric radio communications are affected in two different ways (Carrano, Groves and Caton 2012). The first group of impact is caused by the presence of the background free electrons and their interaction with the signal. Such interactions cause signal loss, phase advance, group delays, distortion and degradation of signal, *etc.* (Alizadeh, et al. 2013). Additionally, a change in the orientation of polarization of an electromagnetic (EM) wave, when traversing through the medium, is experienced in the form of Faraday rotation (FR) angle (Bickel and Bates 1965). The next category of ionospheric effect is due to the interaction of low frequency radio signals with a layer of electron density irregularities, and is termed as ionospheric scintillations (Briggs 1975).

1.2 Ionospheric scintillations

Ionospheric scintillations are defined as modulations in the amplitude (Belcher and Cannon, Amplitude scintillation effects on SAR 2014) and/or phase of the radio signal waveform (Belcher and Rogers, Theory and simulation of ionopsheric effects on synthetic aperture radar 2008). These fluctuations arise due to electron density irregularities that occur in low latitudes because of rapid recombination of free electrons in the bottomside ionosphere after local sunset (Dasgupta, Maitra and Das 1985). The equatorial plasma bubbles formed following the Rayleigh-Taylor instability is the major contributor to scintillations in the equatorial region (Abdu, et al. 2006). At the polar and auroral latitudes, scintillations are present almost every time during the day and are structured by magnetospheric events and solar winds in the form of particle precipitation, plasma processes or E×B drifts (Keskinen and Ossakow, Theories of high-latitude ionospheric irregularities: A review 1983,

* Corresponding author

Keskinen, The structure of high-latitude ionosphere and magnetosphere 1984). The sources and structures of ionospheric scintillations vary over the Earth’s surface. Low latitudes ionospheric irregularities are viewed as rod-like structures aligned with the geomagnetic field lines (C. Rino 1979) while at high latitudes they are viewed as sheet-like structures (Rino, Livingston and Matthews 1978), thus having varied impact on sensors and systems.

1.3 Impact of the ionospheric scintillations on SAR

The interaction of SAR with the ionosphere is a complex two-way process (Carrano, Groves and Caton 2012). When the SAR signal is transmitted from the sensor, it first interacts with the irregularity layer after which the modulated wavefront propagates downwards and interacts with the targets. During the process of transmission, the interaction with irregularities is a diffractive process that modulates the wavefront. Upon return, the wavefront is further modulated after it interacts with the irregularity layer a second time. The time during which SAR transmits and receives the signal is so short that the layer of ionospheric irregularity can be considered to have been unchanged. The size of the irregularities compared to the first Fresnel scale ($\lambda z^{1/2}$, where λ is the wavelength and z is the distance between the target and the layer of irregularity) determines the type of scintillation that the SAR signal is expected to experience (Briggs 1975). When the ionospheric irregularities are larger than the Fresnel zone, the phase scintillations occur (Xu, Wu and Wu 2004). These result in loss of image contrast and blurring of images. Events of phase scintillations are more prevalent at high latitudes compared to equatorial regions. However, when the irregularity scale size is smaller than the Fresnel zone, we have both amplitude and phase scintillation phenomena (Xu, Wu and Wu 2004). SAR sensors flying over low latitudes predominantly experience amplitude scintillations which appear as stripes in the direction of the flight (azimuth) due to diffraction. The intensity and structure of the azimuth streaks in SAR images depend on the orientation of the local magnetic field direction with respect to the flight direction (Meyer, et al. 2016, Kim, et al. 2017).

1.4 Scintillation Monitoring

Monitoring of ionospheric scintillations have widely been carried out by many instruments, such as VHF and beacon receivers (Hunsucker 1991), Global Navigation Satellite System (GNSS) (Morton, et al. 2014), incoherent scatter radars, etc. Among them the most popular technique is using Global Positioning System (GPS) (Ciraolo and Spalla 1997). The standard denotation of describing a scintillation event is in terms of two measurement indices, amplitude scintillation (S_4) (Whitney, Aarons and Malik 1969) and phase scintillation (σ_φ) (Wernik, Alfonsi and Materassi 2007) indices. Similar to GPS/GNSS signals, SAR sensors operating at L-band and P-band can serve as a good tool for observing ionospheric scintillation effects (Pi, et al. 2011).

This work particularly aims at highlighting the capability of SAR, as a complementary technique to GPS/GNSS or ground-based receiver data, in quantitatively characterizing the ionospheric scintillation. This is achieved in describing the scintillation parameters of amplitude scintillation index (S_4) quantitatively. To highlight the improved outreach of SAR for such studies, a small region in Tamil Nadu, in the southern part of India is chosen. Multi-temporal SAR data from Advanced Land Observation Satellite (ALOS)-2 are acquired. The different conditions of ionosphere on dates of SAR data acquisition are established with the help of GPS measurements. The work thus highlights the improving capability of SAR, as a tool, for ionospheric studies which seems to be of extreme importance for current- and upcoming- SAR missions such as ALOS-2 and NISAR respectively.

The organization of the paper is as follows. Details of SAR and GPS data used are explained in Section 2. The two techniques of computing S_4 from SAR is addressed in Section 3. The results are discussed in Section 4 followed by the summary in Section 5.

2. DATASET

2.1 SAR data

Five polarimetric SAR data sets acquired by Advanced Land Observation Satellite-2/Phased Array type L-band Synthetic Aperture Radar (ALOS-2/PALSAR-2) have been used in this study. Under ionospheric scintillation conditions, stripes are visible in one of the SAR intensity image. Comparison of the ionospheric conditions is done with the other four ALOS-2/PALSAR-2 data sets. These data sets have been acquired over a period of 1.5 years over the same area and are shown in Figure 1. The details of the data sets utilized in the study are given in Table 1.

Sl. No.	Scene ID, Polarization, Off-Nadir angle	Date	Ionospheric condition
1.	ALOS2017990170, DP, 28.6º	2014-09-22	Quiet
2.	ALOS2040760170, DP, 32.5º	2015-02-23	Quiet
3.	ALOS2044900170, FP, 30.9º	2015-03-23	Disturbed
4.	ALOS2065600170, DP, 28.6º	2015-08-10	Quiet
5.	ALOS2094580170, DP, 32.9º	2016-02-22	Quiet

Table 1. Details of ALOS-2/PALSAR-2 data sets used

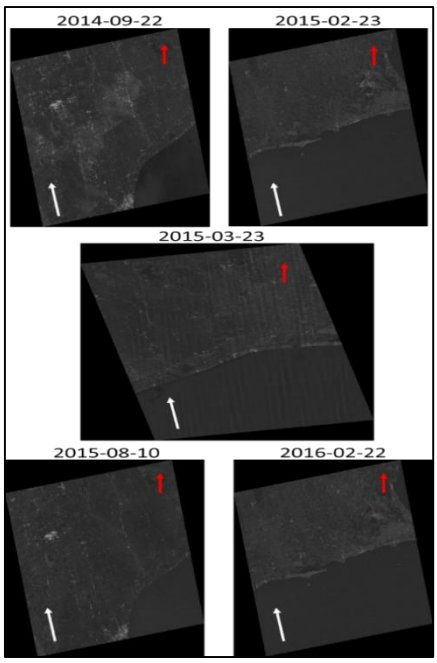

Figure 1. ALOS-2/PALSAR-2 scenes under study. The white and red arrows denote the directions of flight and geographic north respectively

Apart from the third scene on the list (Scene ID: ALOS2044900170) which is fully polarized (HH, HV, VH, VV) all other SAR acquisitions are dual polarized (HH, VV). Also the off-nadir angles of the data sets are different. Since the orbits of the data sets were not completely overlapping, the areas common in the quiet- and disturbed-days are taken into consideration in the study. Prominent stripes can be observed in the third scene, acquired on March 23, 2015, indicating that it was affected by ionospheric scintillation (Shimada, Muraki and Otsuka 2008, Meyer, et al. 2016) while other scenes were not. The usage of the term ionospheric disturbed- and quiet-days are made in context with the levels of scintillations measured using the ground-based GPS receiver station. Total electron content (TEC) and S_4 measurements from GPS satellites from Tirunelveli are used to corroborate the varied ionospheric conditions. These measurements are explained at length in the following subsection. Figure 2 shows the extent of SAR data sets on the ground (after ortho-rectification). The data sets are taken around a small area in the state of Tamil Nadu towards the southern-most tip. The location of the Tirunelveli station is also indicated in the map.

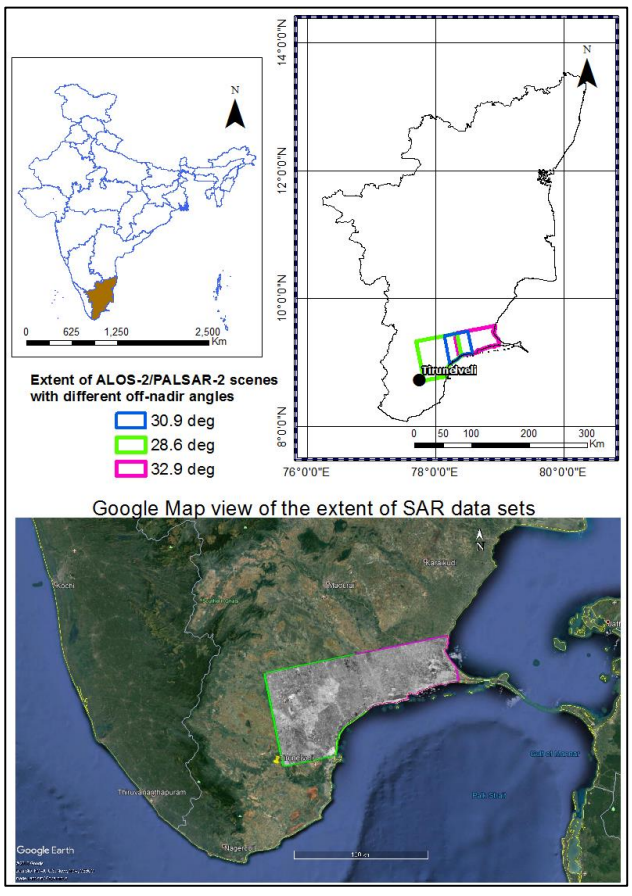

Figure 2. Position of ALOS-2/PALSAR-2 scenes are shown with respect to the ground-station at Tirunelveli. The extents of scenes with different off-nadir angle are also shown.

2.2 Ground-based measurement data

Data from the Tirunelveli scintillation monitoring station under the SCIntillation Network Decision Aid (SCINDA) network (Carrano and Groves 2006) (geographic: 8.67°N, 77.81°E; geomagnetic: 0.17°N, 150.80°E) is utilized to establish the ionospheric conditions on the dates of SAR acquisitions. The measurements of TEC and S_4 also help in validating our results from SAR.

The total number of electrons along the slant range direction between the signal source and the receiver is called as the total electron content (TEC) and is measured in electrons per meter square. One TEC unit (TECU) is equal to 10^{16} electrons/m^2. High density of TEC does not always indicate presence of irregularities leading up to scintillations. Hence we must search for disturbances within the diurnal variation of TEC to identify scintillation events on a particular day.

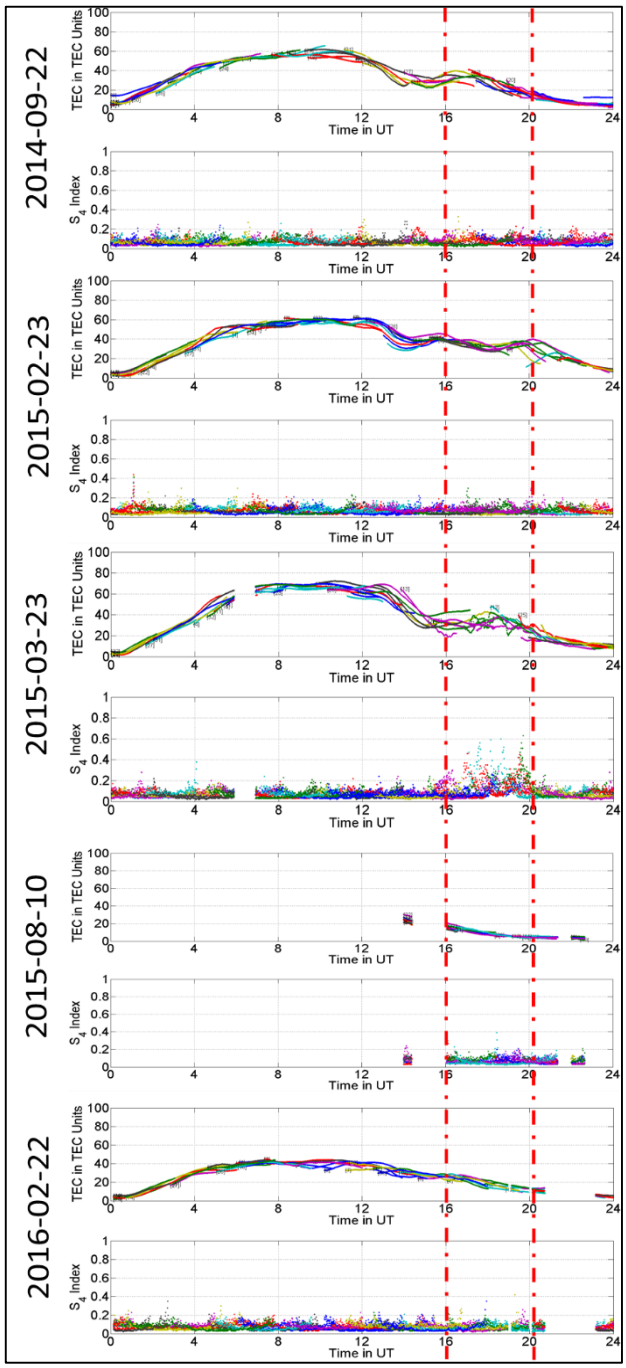

Figure 3. TEC and S_4 plots from GPS satellites observed at Tirunelveli. High scintillation activity can be observed for March 23, 2015

Figure 3 shows the diurnal variation of TEC and the amplitude scintillation index S_4 measured on the dates of SAR acquisition. The red-dotted line from 1600-2000 UT indicates a 4-hour time window within which TEC and S_4 are compared and contrasted. The time of satellite pass is ~ 1900 UT, corresponding to 30 minutes past midnight local time. Ionospheric irregularities originate after local sunset and develop very rapidly within 1-2 hours. As the night progresses, these irregularities fossilize and drift along the east, because of the eastward plasma velocity (in the equatorial region). Thus, by the time SAR observes these irregularities at midnight they may have weakened in intensity. However, on March 23, 2015, the irregularity strength was the highest indicated by the fluctuations in TEC as well as high values of S_4 ~ 0.6.

3. SAR FOR IONOSPHERIC SCINTILLATION OBSERVATION

It has been only recently observed that ionospheric studies using SAR has gained immense importance. SAR sensors, like GPS satellites, operating at low frequencies are severely affected by both amplitude and phase scintillations (Belcher and Cannon, Amplitude scintillation effects on SAR 2014, Belcher and Rogers, Theory and simulation of ionopsheric effects on synthetic aperture radar 2008). Unlike azimuthal stripes that are the initial indication of amplitude scintillation affecting SAR data, SAR affected by phase scintillation have loss of image contrast or defocusing of the image. Previous authors have developed several methods of quantifying ionospheric scintillations in SAR. There are two methods that estimate the strength of amplitude scintillation (S_4 index) (Belcher and Cannon, Amplitude scintillation effects on SAR 2014) while other two methods calculate the strength of turbulence strength (C_KL) (Belcher, Mannix and Cannon, Measurement of the ionospheric scintillation parameter CkL from SAR images of clutter 2017, Mannix, Belcher and Cannon 2017). The point spread function response from point targets, such as corner reflectors, as well as the K-distribution from clutter statistics is used in determining C_KL. With knowledge of the satellite viewing geometry, C_KL can be converted to S_4 (C. Rino 1979). However, in the absence of precise SAR clutter statistics and unavailability of point targets, we use two methods of determining S_4 directly from SAR data in the study. Brief explanation of the two methods are explained below.

3.1 S_4 from radar cross-section (RCS) enhancement

As the name suggests, the RCS enhancement technique depends on the increase in radar cross-section of a homogeneous target during the event of scintillation. Targets with uniform cross-section, under scintillation conditions, have backscatter returns from several directions along with the direct ray beam (Knepp and Houpis 1991). As a result, multiple interferences occur that increase the RCS. The ratio of the mean RCS under conditions of scintillations (μ_{IONO}) to that of under quiet ionospheric conditions (μ) is directly related to the two-way S_{4x2} (Belcher and Cannon, Amplitude scintillation effects on SAR 2014) as

$$\frac{\mu_{IONO}}{\mu^2} = 1 + S_4^2 \tag{1}$$

and the one-way S_4 can be computed to be (Knepp and Houpis 1991)

$$S_{4x2}{}^2 = 4S_4{}^2 + 2\frac{S_4{}^4}{S_4{}^2 + 1} \tag{2}$$

This technique does not depend on any factors, thus giving a direct estimate of S_4. However, the only limitation is that the region of interest (ROI) chosen in the SAR image should have uniform cross-section.

3.2 S_4 from image contrast

The second technique of determining the intensity of amplitude scintillation is using the information of loss of contrast in SAR due to scintillations. Under the assumption that the stochastic sum of amplitude samples in a Fresnel zone determine the amplitude scintillation in SAR, the amplitude of a SAR image is integrated over *N* such independent Fresnel zones. (Belcher and Cannon, Amplitude scintillation effects on SAR 2014) Ratio of the standard deviation to the mean of disturbed- and quiet-day SAR data sets gives the contrast C_d. The equation for estimating one-way S_4 from image contrast is given as

$$S_4^2 = \frac{N}{12}\left(C_d^2 - 4 + 4\sqrt{1 + C_d^2 + \frac{C_d^4}{16}}\right) \tag{3}$$

The determining factor *N* defined as the number of independent Fresnel zones and is given as

$$N = \frac{L_{SA}}{\gamma Z_F} \tag{4}$$

It depends on the length of the synthetic aperture (L_{SA}), the size of the Fresnel zone (Z_F) and γ, defined as the ratio between the spatial distance along the aperture and the effective distance along the phase screen. Details of computing N is given in (Belcher and Cannon, Amplitude scintillation effects on SAR 2014).

4. COMPARISON OF S_4 ESTIMATED FROM SAR AND MEASURED FROM GPS

Results from the above mentioned two techniques of estimating S_4 are reported in this section followed by a comparison with the measurements from GPS satellites. SAR data sets are first calibrated (Motohka, et al. 2018). Since the data sets have different off-nadir (incidence) angles, they are ortho-rectified. To obtain an incidence angle free measure of the SAR return, gamma naught (γ^o) is calculated from the sigma naught (σ^o) the local incidence angle (θ_i) obtained after terrain correction (Woodhouse 2006) as

$$\gamma^0 = \frac{\sigma^0}{\cos\theta_i} \tag{5}$$

The common overlapping area between the SAR data sets are chosen from the data sets with different incidence angles and shown in Figure 4.

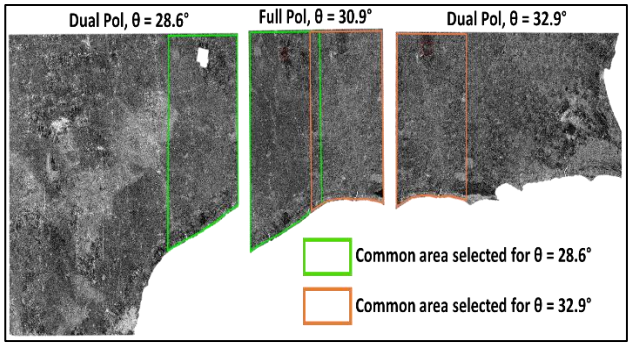

Figure 4. Extent of overlapping areas in data with different off-nadir (incidence) angle.

Region of interest pertaining to the incidence angle of the SAR data sets are extracted. These are shown in Figure 5. To avoid repetitiveness, ROIs from three dates are only shown. After the ROI extraction, first the RCS enhancement technique is applied on the data. To avoid any biasness in the selection of further subsets, the RCS algorithm is applied on the entire ROI. Smaller subsets are made from the bigger ROI where 50 x 25 pixels are chosen in the azimuth and range directions respectively. Ratios of the RCS of these smaller subsets, in both disturbed- and quiet-days, are then computed to calculate the S_4 for that particular image pair.

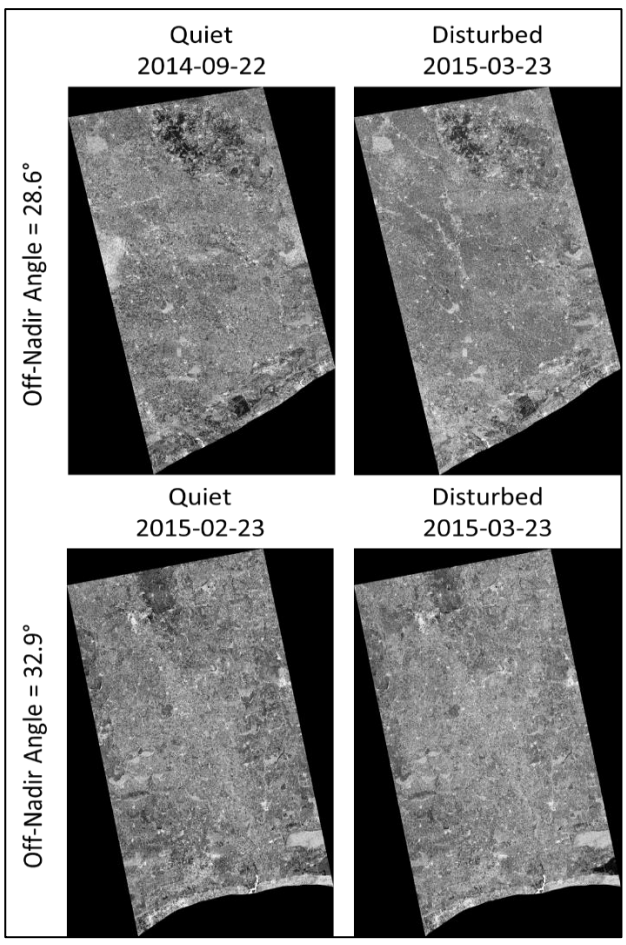

Figure 5. Common region of interest chosen for S_4 estimation

As mentioned earlier in the estimation of S_4 by the contrast method, the number of independent Fresnel zones *N*, is the limiting factor. We have assumed a phase spectral index of 2.5 and an anisotropy factor of 50:1 in the calculation of γ, an input in the calculation of *N*. These values have been chosen taking into account the historical data used in WideBand MODel (WBMOD) (Secan, et al. 1995). Details related to the factor γ and its computation is given in (C. Rino 1979).

Table 2 below presents a comparative analysis of the S_4 estimated from the two techniques for all the SAR pair. Each quiet-day ALOS-2/PALSAR-2 data is paired with the lone disturbed day data, *i.e.*, March 23, 2015 to compute S_4. Thus, there are four pairs of SAR data that are used in the study. The S_4 estimated for the ROIs in each pair demonstrates the strength of the ionosphere on the disturbed day. We can observe that the pairs 1, 3, and 4 have almost similar values compared to the second pair.

Sl. No.	SAR data sets paired with 2015-03-23 data	One-way S_4	
		RCS enhancement	Image Contrast
1.	2014-09-22	0.17	0.16
2.	2015-02-23	0.22	0.23
3.	2015-08-10	0.18	0.2
4.	2016-02-22	0.16	0.17

Table 2. Comparison of S_4 estimated from two methods

The data pair of 2015-02-23 (quiet) and 2015-03-23 (disturbed) have a comparatively higher S_4. This is explained by the small temporal gap of one month between the data sets. In the other pairs the temporal gap varies between 5 months to 11 months. Over this long time gap, one can expect the terrain to have changed. The change in terrain may have hampered the radar cross-section, that is assumed to be constant for the RCS enhancement technique. Moreover, another assumption of a statistically homogeneous ionosphere may also have varied between the different quiet dates considered in study.

The average S_4 measured at Tirunelveli station is 0.21 on March 23, 2015 (Mohanty, et al. 2018). This has been computed taking into account all the satellites observed at the station within a three-hour time window (17:30 to 20:30 UT) and satisfied a criterion. This is referred to as the plasma drift velocity criterion. According to this, measurements from all satellites that have their ionospheric pierce point to the west of the satellite track which must have travelled eastward between 50-150 m/s so as to reach the ALOS-2 track at 1900 UT are included. The same applies to satellites to the east of the SAR track post 1900 UT. Details of measurement of the plasma drift and the selection of GPS satellites to be included in the study are explained and given in (Mohanty, et al. 2018). The slight variation in S_4 measured from GPS and that estimated from SAR pairs is due to the difference in position of the ionospheric pierce points of the satellites and SAR. Latitudinal separation between them may result in both, the GPS receiver and SAR, viewing irregularities at the different stages on their evolution. It may happen so that GPS satellites may have viewed the ionospheric irregularities at an early stage, and by the time they drifted to reach the SAR track the irregularities may have fossilized into finer structures. Nevertheless, we can observe a good agreement between results from both sensors.

This contribution has been peer-reviewed. The double-blind peer-review was conducted on the basis of the full paper.
https://doi.org/10.5194/isprs-annals-IV-5-331-2018 | © Authors 2018. CC BY 4.0 License.

5. SUMMARY

This paper demonstrates the capability of low frequency SAR for observation and quantification of ionospheric scintillations. The scintillation event under study is observed in the southern part of the Indian subcontinent. Coincidently a scintillation monitor from the SCINDA network at Tirunelveli is taken for validating the S_4 measurements from SAR. ALOS-2/PALSAR-2 data sets over this region is obtained over one and half years to create data pairs. As multi-temporal SAR data are useful in drawing conclusion about the surface backscatter, likewise these data pairs help us infer about the condition of ionosphere. Results of S_4 measurements from SAR are well corroborated with those from the ground-based scintillation monitor. S_4 estimated with the data pair having the smallest temporal gap has a good agreement with ground measurements. Furthermore, with precise information of satellite viewing geometry, we can also estimate the strength of turbulence which is an inherent property of the ionospheric medium independent of satellite geometry. With many low frequency SAR missions coming up in the future, we can implement these well-established techniques for quantifying ionospheric scintillations.

ACKNOWLEDGEMENTS

The authors express their gratitude to JAXA for providing the data sets under RA6 Project 3169. The authors also thank Christopher Bridgwood, ISR, Boston College for providing the TEC and S_4 measurements at Tirunelveli.

REFERENCES

Abdu, M.A., K.N. Iyer, R.T. de Medeiros, I.S. Batista, and J.H.A. Sobral. 2006. “Thermospheric meridional wind control of equatorial spread F and evening prereversal electric field.” *Geophysical Research Letters* 1-4. doi:10.1029/2005GL024835.

Alizadeh, M. M., D. D. Wijaya, T. Hobiger, R. Weber, and H. Schuh. 2013. “Ionospheric Effects on Microwave Signals.” In *Atmospheric Effects in Space Geodesy. Springer Atmospheric Sciences*. Berlin: Springer. doi:10.1007/978-3-642-36932-2_2.

Belcher, D.P., and N.C. Rogers. 2008. “Theory and simulation of ionopsheric effects on synthetic aperture radar.” *IET Radar Sonar Navig.* 541-551. doi:10.1049/iet-rsn.2008.0205.

Belcher, D.P., and P.S. Cannon. 2014. “Amplitude scintillation effects on SAR.” *IET Radar Sonar Navig.* 658-666. doi:10.1049/iet-rsn.2013.0168.

Belcher, D.P., C.R. Mannix, and P.S. Cannon. 2017. “Measurement of the ionospheric scintillation parameter CkL from SAR images of clutter.” *IEEE Trans. Geoscience and Remote Sensing* 5937 - 5943. doi:10.1109/TGRS.2017.2717081.

Bickel, S. H., and R. H.T. Bates. 1965. “Effect of magneto-ionic propagation on polarization scattering matrix.” *Proceedings of the IEEE* 53 (8): 1089-1091. doi:10.1109/PROC.1965.4097.

Briggs, B. H. 1975. “Ionospheric irregularities and radio scintillations.” *Contemporary Physics* 16 (5): 469-488. doi:10.1080/00107517508210825.

Cannon, Paul, and et al. 2013. *Extreme space weather: impacts on engineered systems.* London, UK: Royal Academy of Engineering.https://www.raeng.org.uk/publications/reports/space-weather-full-report.

Carrano, C. S., C. T. Bridgwood, and K. M. Groves. 2009. “Impacts of the December 2006 solar radio bursts on the performance of GPS.” *Radio Science* 44 (RS0A25): 1-12. doi:10.1029/2008RS004071.

Carrano, C., and K.M. Groves. 2006. “The GPS Segment of the AFRL-SCINDA Global Network and the Challenges of Real-Time TEC Estimation in the Equatorial Ionosphere.” *National Technical Meeting of the Institute of Navigation.* Monterey, CA. 1036-1047.

Carrano, C.S., K.M. Groves, and R.G. Caton. 2012. “Simulating the impacts of ionospheric scintillation on L band SAR image formation.” *Radio Science* (Radio Science) 47 (7): 1-14. doi:10.1029/2011RS004956.

Ciraolo, L., and P. Spalla. 1997. “Comparison of ionospheric total electron content from the Navy Navigation Satellite System and the GPS.” *Radio Science* 1071-1080. doi:10.1029/97RS00425.

Dasgupta, A., A. Maitra, and S. K. Das. 1985. “Post-midnight equatorial scintillation activity in relation to geomagnetic disturbances.” *Journal of Atmospheric and Terrestrial Physics* 47 (8-10): 911-916. doi:10.1016/0021-9169(85)90067-4.

Hunsucker, R.D. 1991. “Satellite, Rocket, and Other Techniques.” In *Radio Techniques for Probing the Terrestrial Ionosphere*, by R.D. Hunsucker, 185-228. Berlin, Heidelberg: Springer. doi:10.1007/978-3-642-76257-4.

IEEE, Std 211-1997. 1998. “IEEE Standard Definitions of Terms for Radio Wave Propagation.” *IEEE Std 211-1997.* doi:10.1109/IEEESTD.1998.87897.

Keskinen, M. J. 1984. “The structure of high-latitude ionosphere and magnetosphere.” *John Hopkins APL Technical Digest* 5 (2): 154-158.

Keskinen, M. J., and S. L. Ossakow. 1983. “Theories of high-latitude ionospheric irregularities: A review .” *Radio Science* 18 (6): 1077-1091.

Kim, Jun Su, K.P Papathanassiou, H. Sato, and S. Quegan. 2017. “Detection and estimation of equatorial spread F scintillations using synthetic aperture radar.” *IEEE Trans. Geosci. Remote Sens.* 55 (12): 6713-6725. doi:10.1109/TGRS.2017.2731943.

Knepp, D.L., and H.L.F. Houpis. 1991. “ALTAIR VHF/UHF observations of multipath and backscatter enhancement.” *IEEE Transactions on Antennas and Propagation* 528-534. doi:10.1109/8.81467.

Mannix, C.R., D.P. Belcher, and P.S. Cannon. 2017. “Measurement of ionospheric scintillation parameters from SAR images using corner reflectors.” *IEEE Trans. Geoscience and Remote Sensing* 1-8. doi:10.1109/TGRS.2017.2727319.

Meyer, F.J., K. Chotoo, S.D. Chotoo, B.D, Huxtable, and C.S. Carrano. 2016. “The influence of equatorial scintillation on L-band SAR image quality and phase.” *IEEE Trans. Geosci. Remote Sens.* 54 (2): 869-880. doi:10.1109/TGRS.2015.2468573.

Mohanty, S., G. Singh, C. S. Carrano, and S. Sripathi. 2018. “Ionospheric scintillation observation using space-borne synthetic aperture radar (SAR) data.” *Radio Science* (accepeted). doi:10.1029/2017RS006424.

Morton, Yu, Dongyang Xu, Mark Carroll, Yu Jiao, Jun Wang, Steve Taylor, and Xiaolei Mao. 2014. “Multi-constellation and multi-frequency GNSS studies of ionospheric scintillation.” *Radio Science Meeting (USNC-URSI NRSM), 2014 United States National Committee of URSI National.* Boulder, CO: IEEE. doi:10.1109/USNC-URSI-NRSM.2014.6928060.

Motohka, T., O. Isoguchi, M. Sakashita, and M. Shimada. 2018. *ALOS-2 PALSAR-2 Cal/Val Updates.* JAXA/EORC Joint PI Meeting of Global Environment Observation Mission FY2017.

Pi, Xiaoqing, Anthony Freeman, Bruce Chapman, Paul Rosen, and Zhenhong Li. 2011. “Imaging ionopsheric inhomogeneities using spaceborne synthetic aperture radar.” *Journal of Geophysical Research: Space Physics* 116 (A4): 1-13. doi:https://doi.org/10.1029/2010JA016267.

Rino, C. L., R. C. Livingston, and S. J. Matthews. 1978. “Evidence for sheet-like auroral ionopsheric irregularities .” *Geophysical Research Letters* 5 (12): 1039-1042.

Rino, C.L. 1979. “A power law phase screen model for ionospheric scintillation: 1. Weak scatter.” *Radio Science* 1135-1145. doi:10.1029/RS014i006p01135.

Secan, J. A., R. M. Bussey, E.J. Fremouw, and Sa Basu. 1995. “An improved model of equatorial scintillation.” *Radio Science* 30 (3): 607-617. doi:10.1029/94RS03172.

Shimada, M., Y. Muraki, and Y. Otsuka. 2008. “Discovery of anomalous stripes over the Amazon by the PALSAR onboard ALOS satellite.” *IEEE International Geoscience and Remote Sensing Symposium (IGARSS).* Boston, MA: IEEE. doi:10.1109/IGARSS.2008.4779009.

Wernik, A.W,, L. Alfonsi, and M. Materassi. 2007. “Scintillation modeling using in situ data.” *Radio Science.* doi:10.1029/2006RS003512.

Whitney, H.E., J. Aarons, and C. Malik. 1969. “A proposed index for measuring ionospheric scintillations.” *Planetary and Space Science* 1069-1073. doi:10.1016/0032-0633(69)90114-7.

Woodhouse, Iain H. 2006. *Introduction to Microwave Remote Sensing.* Boca Raton, FL: CRC Press.

Xu, Z.-W., J. Wu, and Z.-S. Wu. 2004. “A survey of ionospheric effects on space-based radar.” *Waves in Random Media* S189–S273. doi:10.1088/0959-7174/14/2/008.